Proceedings of the
Annual Stability Conference
Structural Stability Research Council
Atlanta, Georgia, April 21-24, 2026

Understanding the effect of modelling methodology on the numerical stability assessment of open web steel joists

Hans E. Lagerquist[1], Pedram Mortazavi[2]

Abstract
Open web steel joists are efficient built-up steel members that are widely used in long-span roof and floor systems. Due to their slender cross section geometry, they are particularly susceptible to lateral-torsional buckling prior to the installation of erection bracing. While the Minkoff–Galambos equation is commonly used in practice to estimate joist capacity, finite element analysis could be used to assess the capacity of joists that fall outside the typical limits of the equation. The behavior of unbraced joists and their lateral torsional buckling capacity are highly sensitive to modelling assumptions including the representation of double-angle chords and the inclusion of filler elements, among other parameters. This study evaluates several finite element modelling approaches in Abaqus, including single beam element, double beam element, hybrid shell–beam, and full shell element models. Each approach is evaluated and verified using experimental data from a previously tested benchmark joist referred to as the 32LH06 joist. Linear buckling and nonlinear analyses were performed to assess the influence of modelling assumptions on joist capacity. The results indicate that the adopted modelling methodology has a substantial effect on predicted capacity, with beam element models generally overestimating strength relative to shell-based models. Recommendations for modelling open web steel joists for stability analysis are provided based on these findings.

1. Introduction

1.1 Background

Open web steel joists (OWSJs) are widely used in long-span applications due to their material efficiency, light weight, and cost-effectiveness. An example application of OWSJs is shown in Figure 1. OWSJs are typically formed by double angle sections in the top and bottom chords, while the internal web members are composed of a variety of sections including rods, single angles, or cold-formed channels. OWSJs are typically designed to support corrugated steel decks with or without concrete topping, while the OWSJs themselves are supported by girders. Joists are connected to the girders through the joist seat shown in Figure 1 (b). The joist seat is typically formed by two angles and is welded to the end of the top chord, similar to that shown in Figure 1 (b). In some cases, the joist bottom double angles sandwich a fin plate welded to the support, referred to as the stabilizer. An example detail is shown in Figure 1 (c). The stabilizer, which can

[1] Graduate Research Assistant, University of Minnesota – Twin Cities, <lager099@umn.edu>
[2] Assistant Professor, University of Minnesota – Twin Cities <pmortaza@umn.edu>

only be used at the column location, is primarily relevant during joist erection and is intended to increase the lateral torsional buckling (LTB) capacity of the joist. The geometry of each joist is optimized for a specific span, depth, and load rating, assuming lateral support along the top chord. While this allows efficient resistance to vertical loads, the slender sections are highly prone to LTB during erection prior to deck placement or installation of bridging.

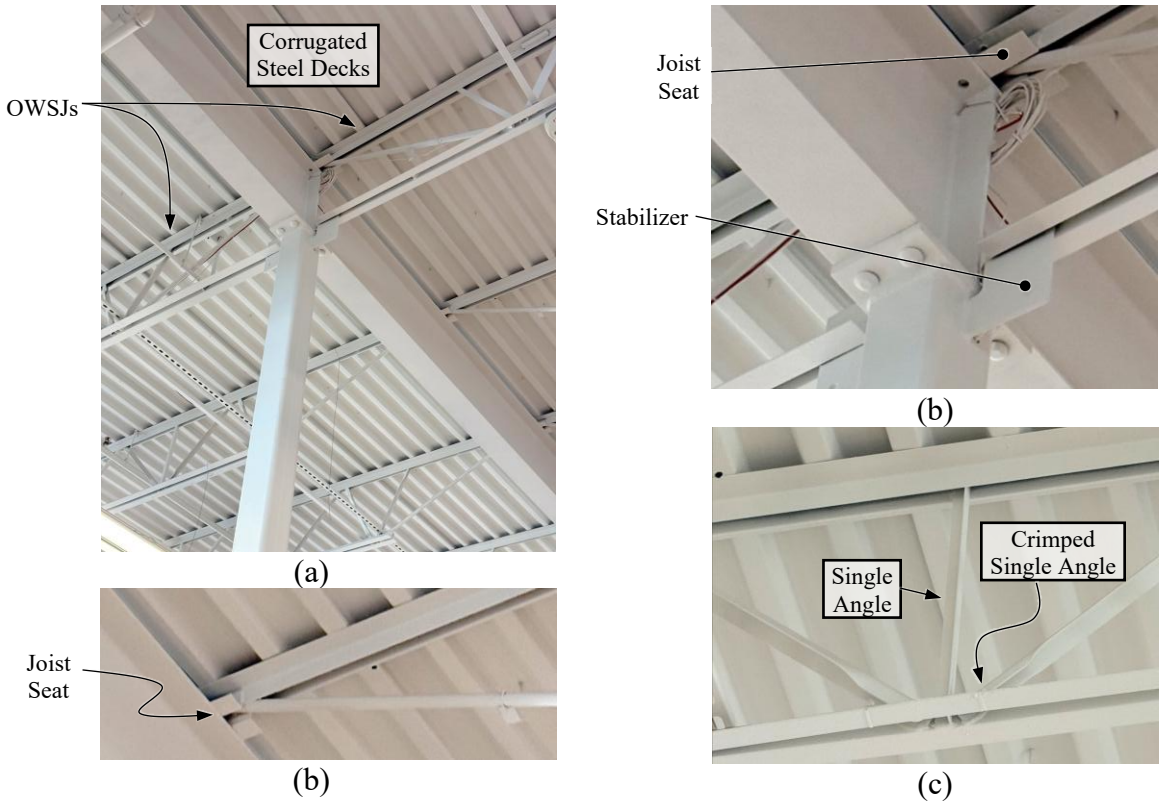

Figure 1: Example Illustration of OWSJs and Relevant Details: (a) OWSJs and their components, (b) Joist Seat, (c) Stabilizer, and (d) Web Members with and without Crimped Angles

Lateral bracing, or erection bridging, is often used during construction to limit out-of-plane deflection. The Steel Joist Institute (SJI) Standard Specifications (2020) provides guidance on the placement and type of bridging. Joists longer than 60 feet always require bridging, while the LTB capacity of joists with shorter spans may be evaluated using the modified Minkoff-Galambos equation (Minkoff, 1975; Galambos, 1993) to determine the critical buckling load. The accuracy of the Minkoff-Galambos equation has been evaluated through experimental testing of joists with varying spans and depths, including assessments of end connections and stabilizer fins (Schwarz, 2002; Emerson, 2001; Ziemian et al. 2004). Results indicated that the equation provides reasonably conservative predictions. However, finite element analysis (FEA) has also been used for evaluating the LTB capacity of OWSJs in both research applications and special case studies in practice. The accuracy of numerical simulations is heavily dependent on the modelling assumptions. As such, it is important to critically evaluate the implications of different modelling assumptions on the accuracy of numerical models for assessing the capacity of OWSJs.

1.2 Previous Numerical Studies on OWSJs

Schwarz (2002) used FEA using MASTAN2 (Ziemian et al., 2019) to predict the LTB capacity of OWSJs. Each joist was modelled using line elements. Second-order geometric effects were considered in the analysis. Out-of-plane bending and torsional stiffness at the supports were incorporated using calibrated beam elements to represent the connection behavior and node positions along the top chord were adjusted to capture the measured lateral sway. Although this methodology was relatively accurate for shorter spans, errors were observed for joists over 40 feet long. Eberle et al. (2012) refined the modelling approach and demonstrated that improved improvements could be made. These studies established a framework for evaluating bracing requirements and predicting lateral stability in full-scale joist systems.

Rojahn and Ziemian (2021) examined the use of other modelling methodologies to capture the lateral-torsional buckling behavior of OWSJs. Two joist designs, 32LH06 and 30K12, were analyzed using both MASTAN2 (Ziemian et al., 2019) and Strand7 (2020) with multiple modelling approaches, including combinations of beam and shell elements. Linear buckling analysis revealed that representing the double angle chords with two parallel beam elements connected by 1-inch filler rods reproduced the results of full shell element models. The number and stiffness of filler elements were found to strongly influence the predicted capacity of the joists. The use of more torsionally stiff fillers increased the capacity of a joist model with a double beam element chord. These findings provided an improved methodology for modelling OWSJs within MASTAN2 and Strand7.

The dual beam element modelling methodology has been applied in subsequent studies to examine lateral stability under varying conditions. Moore (2024) investigated flush frame connections using experimental testing and numerical modelling, employing boundary elements to represent lateral and torsional stiffness of the connection. Linear buckling analysis was used to calibrate models against calculated critical buckling loads from experiments. Ward (2025) applied a similar approach to double-pitched OWSJs, using idealized boundary conditions in the absence of experimental data, which were found to be conservative for stability assessment.

1.3 Paper Objective and Layout

The objective of this study is to provide a comprehensive evaluation of modelling methodologies for OWSJs, and to understand the effects of modelling assumptions on results from FEAs. The numerical models and simulations are developed and performed in Abaqus (2023). However, the findings may be directly transferable to other commonly used finite element packages. Different numerical modelling approaches for capturing the response of OWSJs are presented in detail. The results from each modelling approach are compared with experimental results on the benchmark joist (i.e., 32LH06 joist) from a previous study. The advantages and limitations of each modelling approach are critically evaluated. Section 2.0 presents the OWSJs used in the present study. Section 3.0 details the numerical modelling approaches and detailed assumptions used in each modelling approach. Prior to presenting detailed results from the numerical model, the effects of several assumptions such as initial camber (i.e., vertical camber), initial lateral sway, and the size of the double chord filler elements on the response are discussed in Section 4.0. A detailed comparison between results obtained using different modelling approaches is presented in Section 5.0. Concluding remarks and recommendations for future studies are provided in Section 6.0.

2. Reference Open-Web Steel Joists

For this study, the OWSJs tested by Schwarz (2002) were selected due to the comprehensive experimental data available. Table 1 lists the joists used in the study along with their reference designations and Fig. 2 displays two of the joists examined, along with a display of the relevant terminology. Member sections are provided in Table 2. The selected joists included a series of OWSJs including a reasonable range of span lengths, chord dimensions, and web geometries. This allows for a comprehensive assessment of modelling assumptions across different joist configurations. The joist capacity was primarily evaluated at a lateral deformation of 5.7 in, which corresponds to the L/120 deflection limit with L being the length of the joist.

Table 1: Reference OWSJ Information from Schwarz (2002)

Joist Designation	Span Length	Joist Weight (lb)	Max. Out-of-Straightness	L/Imperfection	Joist Designation (Schwarz, 2002)
10K1	19'-10"	97	1/4"	952	J8_10K1
18K3	28'-3"	165	7/16"	775	J10_18K3
26K5	37'-3.5"	295	13/16"	551	J12_26K5
28K10	48'-3"	573	1-7/8"	309	J13_28K10
32LH06	57'-0"	848*	1-3/4"	391	L2_32LH06

**Information not provided within Schwarz (2002). Weight was calculated using geometric information.*

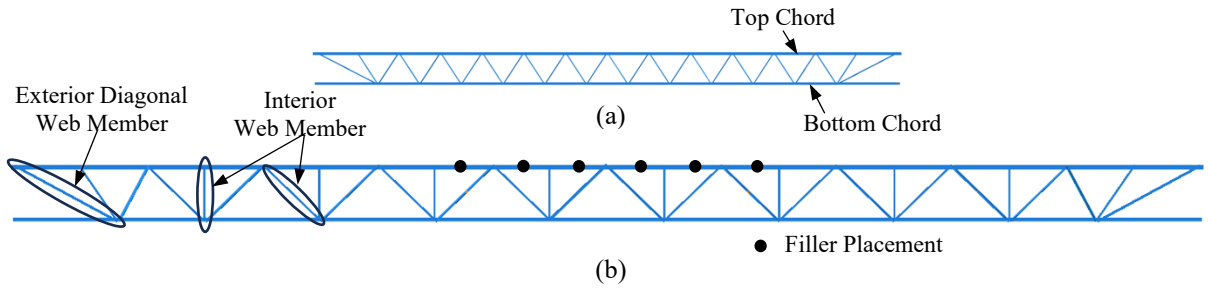

Figure 2: Schematic illustration of OWSJs tested by Schwarz (2002): (a) Shorter Span Joist with Rod Webs and no Fillers (18K3 shown), and (b) Longer Span Joist with a Variety of Web Members and Fillers (32LH06 shown)

Detailed information regarding the placement or composition of fillers between the top chords is not available in Schwarz (2002). As such, reasonable assumptions were made based on prior studies (Rojahn, 2021; Moore, 2024). Fillers are assumed to be only present for joists longer than 30'. For shorter joists no fillers are provided, and the double chord sections are connected solely at the web/chord intersections. For joists longer than 30', fillers are placed at the midspan of chord panels, only for the panels within the mid-span of the joist. A visualization of the placement of the fillers is shown in Fig. 2 (b).

In addition to geometric and material properties, load-deflection measurements from the experiments were used to evaluate and verify the modelling approaches. Measured out-of-straightness values obtained from the testing program were used to define the initial geometric imperfections in the models, which are critical for accurately capturing stability-related behavior in OWSJs. The 32LH06 joist is used as the primary benchmark joist for verifying the modelling methodologies with experimental results. The same modelling approach is then used for the other reference joists without verification with experimental results.

Table 2: Double Angle Chord Dimensions and Web Member Composition

Joist Designation	Top Chord Section	Top Chord Thickness	Bottom Chord Section	Bottom Chord Thickness	Chord Spacing	Web Member Style
10K1	(2) 1.5×1.5	0.123	(2) 1×1	0.109	0.5	Round
18K3	(2) 1.5×1.5	0.123	(2) 1.25×1.25	0.109	0.5	Round
26K5	(2) 1.75×1.75	0.155	(2) 1.5×1.5	0.123	1	Varies
28K10	(2) 2×2	0.24	(2) 2×2	0.163	1	Varies
32LH06	(2) 2.5×2.5	0.212	(2) 2×2	0.216	1	Angles

All dimensions in inches

3. Numerical Modelling Methodologies

Four modelling approaches are studied using a combination of beam elements and/or shell elements. A summary of the numerical modelling approaches is presented in Table 3. An illustration the models is also shown in Fig. 3. The modelling approaches include: (1) the Single Beam Element (SBE) Model, (2) the Double Beam Elements (DBE) Model, (3) the Hybrid Element (HE), and (4) the Shell Element (SE) Model. The SE model, which is the highest fidelity model and more computationally demanding, was only developed and evaluated for the benchmark 32LH06 joist.

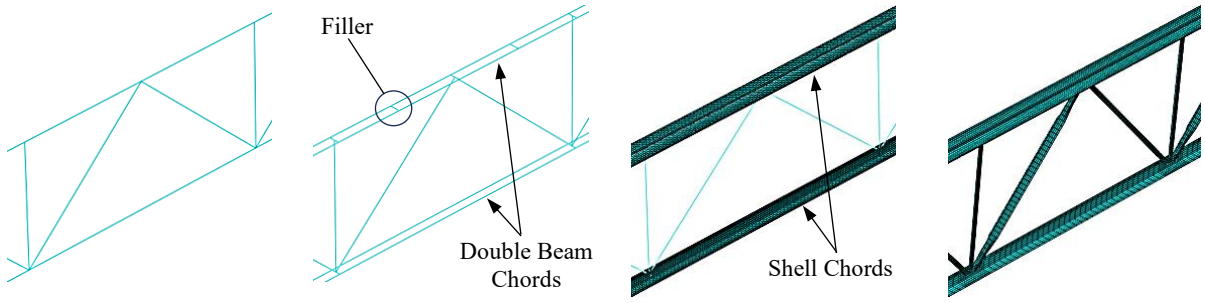

Figure 3: Modelling Approaches: (a) Single Beam Element (SBE), (b) Double Beam Element (DBE), (c) Hybrid Element (HE), (d) Shell Element (SE)

For all models summarized in Table 3, linear buckling analysis (LBA) was performed first to determine the primary buckling mode shape for the laterally unbraced joist. In all instances a failure mode of LTB was found. This mode shape was then used to define the initial imperfection shape in the finite element models. The finite element models were then used to impose a monotonic point load at midspan on the joists, while considering both material and geometric nonlinearities. In addition to the applied point load, a gravity load based on material density was applied prior to load incrementation. The selected load application replicates the experimental conditions reported by Schwarz (2002).

Each model was created with a pin support at one end and a roller support at the other end of the top chord, to ensure no axial restraint or second-order effects were imposed on the joists. In addition to the simply supported conditions, rotation about the longitudinal axis of the joist was restrained to replicate the restraint provided by the bearing joist seat in typical OWSJs. The bottom chord was restrained laterally at its end to simulate the inclusion of a stabilizer plate (Schwarz 2002).

Material properties of the joists were not explicitly documented in Schwarz (2002). Accordingly, nominal material properties were assumed for all models, including a yield strength of 36 ksi (250 MPa) and an elastic modulus of 29,000 ksi (200 GPa). The material nonlinearity was assumed to be based on typical stress-strain response A36 steel.

Table 3: Summary of Modelling Methodologies

Model Type	Description
Single Beam Element (SBE)	All joist components modelled with single beam elements.
Double Beam Element (DBE)	Top chord, bottom chord, and all double angle web members modelled with two parallel beam elements representing the angle sections. The chord double angles were connected by beam element fillers. All other web members with single angles were modelled with single beam elements.
Hybrid Element (HE)	Top and bottom chords modelled with shell elements, with the top chord double angles connected by beam element fillers. Web members modelled with single beam elements.
Shell Element (SE)	All joist components with an angle section modelled with shell elements. All joist components with rod sections modelled using solid elements.

In the present study, the numerical models using each approach are verified with experimental results for the benchmark 32LH06 joist. This joist was chosen as the main reference joist given its longer span and its higher susceptibility to lateral torsional buckling. Application of the methodologies to the remaining joists is discussed in subsequent sections.

3.1 Single Beam Element (SBE) Model

In the single beam element modelling approach, all joist members were represented using beam elements within Abaqus. Cross-sectional properties for the chord members were defined using the arbitrary cross-section tool in Abaqus, which enables the creation of general thin-walled sections and facilitates computing the associated sectional properties. A discussion of the impact of the section definition method is discussed in Section 4.1. The section properties were defined about the shear center to remain consistent with Abaqus default section definition for angle sections and to ensure that torsional response was appropriately captured. Chord members and angle section web members were modelled using B31OS beam elements, which account for the behavior of open sections and include warping effects in torsion. The point load was applied directly to the node at midspan, and the boundary conditions were applied directly to the nodes at the joist ends.

3.2 Double Beam Element (DBE) Model

The double beam element model was developed by Rojahn and Ziemian (2021) to provide a more refined representation of the double-angle chord behavior while maintaining the computational efficiency of beam-based formulations. In this approach, each chord member was modelled using two parallel beam elements, with each beam representing one angle of the double-angle chord. The parallel chord elements were connected by a series of short filler elements, intended to represent both the discrete connectors used in physical joist construction, and the stiffness of the chord-web connection.

Filler elements were placed at all chord/web intersection points, as well as at typical filler locations similar to those indicated in Fig.3 (b). These filler elements also served as the connection mechanism between the chord members and the web members. All web members were aligned

along their centerlines and connected directly to the filler elements, thereby establishing load transfer between the web system and the parallel chord elements. The filler elements were modelled as short beam elements and connected to the chord elements using standard node-to-node frame connections. This connection strategy was selected to limit modelling complexity while maintaining compatibility with the beam-based formulation.

Similar to the SBE methodology, all angle section members were modelled using B31OS beam elements. All filler sections modelled as round bars were represented using B31 beam elements, as warping effects are not applicable for these sections. The mid-span point load on the top chord was divided into two-point loads and applied to the midspan nodes of the two beam elements representing the top chord. This approach was selected to more closely mimic the actual loading procedure. The boundary conditions were applied through the use of a rigid tie constraint to a reference point placed at the center of the two chord end nodes.

3.3 Hybrid Element (HE) Model

Hybrid shell-beam models have been previously used by Rojahn and Ziemian (2021) as a modelling methodology intended to balance the higher fidelity of shell models with the computational efficiency of beam elements. In this approach, chord members are modelled using shell elements to more accurately capture local behavior, while web members and auxiliary components are represented using beam elements. This allows the model to account for localized effects in the chords while maintaining reasonable computational cost.

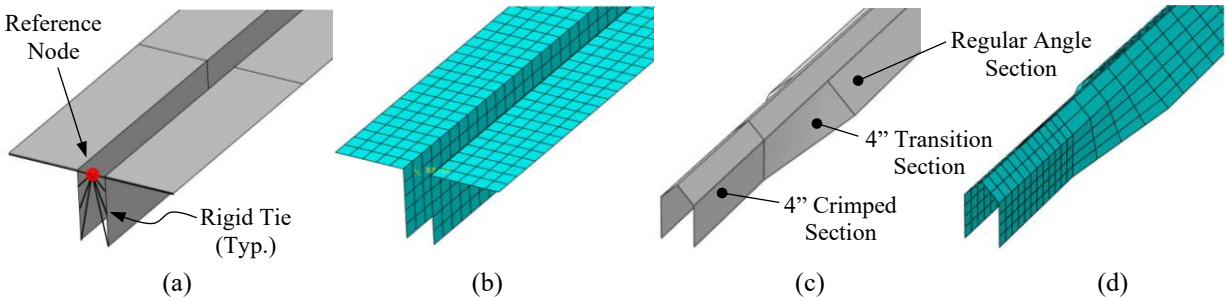

Figure 4: Selected Illustrations from FEAs: (a) Top Chord Geometry and Rigid Tie Constraint in HE and SE Models, (b) Top Chord Mesh Topology in HE and SE Models, (c) Crimped Web Angle Geometry in SE Models, and (d) Crimped Web Angle Mesh Topology in SE Models

In the hybrid shell-beam models developed for this study, the top and bottom chord angles were modelled using S4R shell elements, while all web members and filler elements were modelled using B31, for rod and filler members, and B31OS beam elements, for double and single angle members. This approach is consistent with section definitions employed in beam-only models. The filler elements were positioned at 0.5 inches below the top of the chord, and web members were connected directly to the filler elements. For both shell element modelling methodologies, the midspan point load was applied at the heel of each top chord angle to minimize local warping effects associated with torsional loading at the angle section tips. Boundary conditions were applied to a reference node which was constrained to the entirety of the end of the double angle chords with a rigid tie constraint, similar to that shown in Fig. 4 (a). The boundary condition was then applied to the reference node. The chord mesh topology is shown in Fig. 4 (b), which was defined by placing 5 elements along each angle leg. This element size was maintained throughout the top and bottom chords to create a consistent mesh definition and ensure accurate results.

3.4 Shell Element (SE) Model

The SE modelling approach represents the most detailed and computationally demanding methodology examined in this study. This method used a similar modelling procedure to that discussed in Cicek et al. (2024). In this approach, all angle sections used S4R shell elements to explicitly capture the geometry and deformation behavior of the chord and web members. Filler elements placed between the chord members used C3D8R solid elements.

The crimped portions of single-angle web members were explicitly represented in the shell models. The transition to the crimped region was assumed to begin at a distance of eight inches from the ends of the member. An example of the crimped model is shown in Fig. 4 (c). Connections between the web members and chord members were modelled using surface-to-surface tie constraints

Filler elements were initially placed along the top chord at the locations indicated in Fig. 2 (b), so as to fully replicate the placement seen within a typical joist. In addition to this base configuration, a second shell model was developed in which filler elements were placed at all chord/web intersections, in addition to the standard filler placement locations. This alternative placement strategy was examined to assess the sensitivity of the shell model response to filler location. An example of these configurations is shown in Fig. 5 (a). To further investigate this behavior, an additional model was developed with a continuous filler element placed between the chord members. This continuous filler was modelled as a one-inch thick plate, using shell elements and was tied to both chords to prevent relative motion. The continuous filler element was positioned 0.5 inches below the top of the chord to replicate the other filler application. A visualization of this configuration provided in Fig. 5 (c).

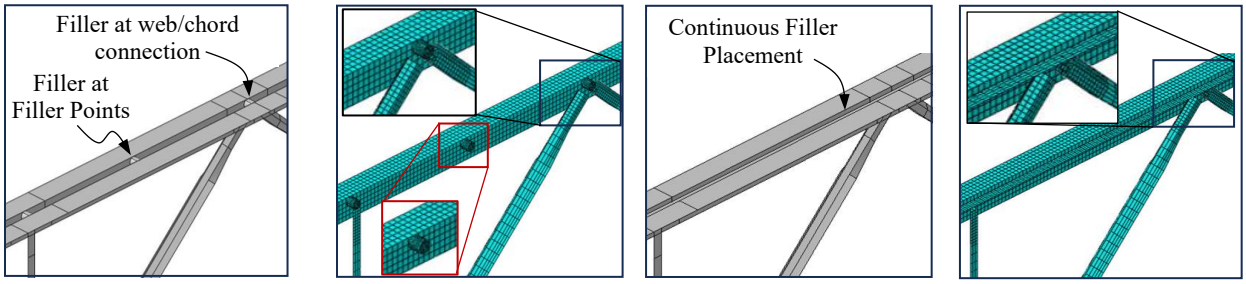

Figure 5: Shell Element Model Filler Placement with (a) Solid Element Rod Fillers and (b) Continuous Shell Element Fillers

The mesh topology for the SE models was more complex than for the HE models due to explicit representation of web member and filler geometries. The chord mesh was done in a similar manner as the HE models. For single-angle web members, the mesh was refined to place a minimum of three elements along each edge of the crimped angle at the chord connection, with a similar meshing strategy applied to uncrimped single-angle and double-angle web members. The meshing topology for a crimped single angle web member is shown in Figure 4 (d). To limit computational cost while maintaining accuracy near connections, the longitudinal mesh density of web members was gradually coarsened, with element lengths increased at a distance of four inches from the web member ends. The mesh topology for the SE models is shown in Figures 5 (b), for the SE model with fillers, and in Figure 5 (d), for the SE model with the continuous filler.

4. Impact of Modelling Assumptions

In addition to the core modelling methodologies examined as a part of this study, a series of other assumptions in modelling OWSJs were examined due to their potential impact on the modelling results. These parameters were examined using the 32LH06 benchmark joist to establish consistent modelling practices prior to application to the remaining reference OWSJs.

4.1 Impact of Beam Section Definition

As previously noted, the combined double-angle chord section in the SBE model was defined using the arbitrary cross-section tool in Abaqus. A limitation of this tool is the requirement that the section geometry be represented as a single continuous profile. To satisfy this requirement, the backs of the two angles were connected by a thin linking segment with a thickness of 0.0004 in. Although introduced solely to ensure geometric continuity, the placement of this connector has the potential to influence the LTB response of the joist. To quantify this effect, four alternative section definitions were investigated, as illustrated in Fig. 6 (a). These configurations varied the vertical placement of the connecting segment relative to the angle geometry.

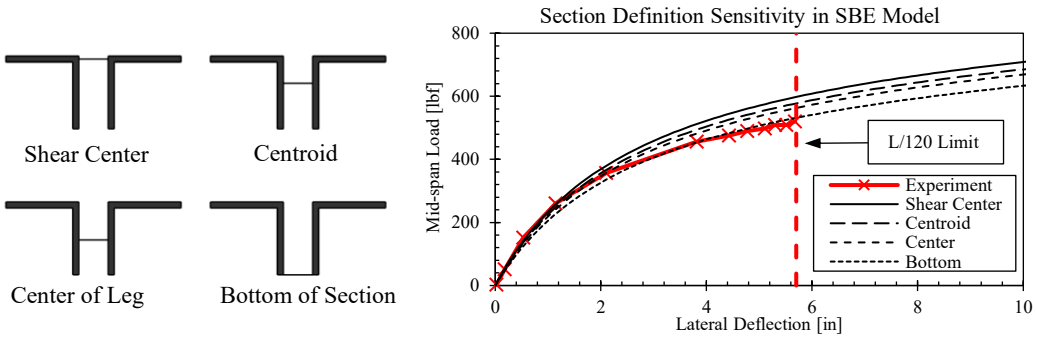

(a) (b)

Figure 6: (a) Singe Beam Element Model Double Angle Section Definition and (b) Load Deflection Plot from Section Definition Investigation

The results from all FEAs using SBE models with different section definitions are shown in Fig. 6 (b) and compared with experimental results from Schwarz (2002). The joist capacity was evaluated at the lateral deformation of 5.7 in (i.e., the *L*/120 deflection limit). As illustrated, the connector section placement can notably affect the predicted joist capacity. When the thin linking segment is placed between the angle section shear centers, the capacity is highest. As the connector moves closer to the section bottom, the capacity reduces and approaches the experimental results more closely. Moving the linking segment across the section height can increase the estimated capacity by 6%. Therefore, the *bottom of section* definition was selected for all other joist models using the SBE, as it matched the experimental results most closely.

4.2 Impact of Camber

Camber is required prescriptively by the SJI Standard Specifications (2020) for OWSJs. This camber is commonly neglected during the finite element modelling process due to the increased complexity that results from considering the non-straight members. However, camber increases the vertical offset between applied loads and the end seats at midspan, potentially introducing additional destabilizing moments due to both self-weight and applied point loads. An example of a cambered joist is shown in Fig. 7. The impact of camber on the capacity of the 32LH06 joist was examined through the creation of an additional SBE model and HE model. An initial camber of 1

3/8” was applied to each model as selected via interpolation from SJI Table 4.6-1. Comparisons between cambered and uncambered configurations are shown in Fig. 8.

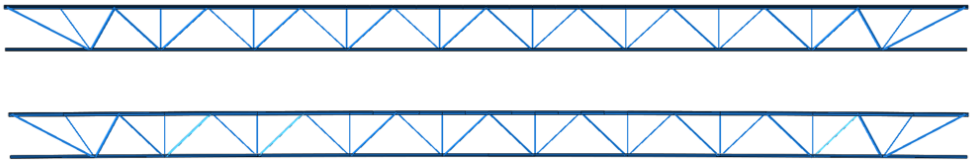

Figure 7: Uncambered 32LH06 Joist Model (Top) and Cambered 32LH06 Joist Model (Bottom)

The joist models were observed to have a small reduction in capacity and stiffness of approximately 3%, when the camber was explicitly considered in the model. Due to the substantial increase in modelling effort required for capturing the camber and given its negligible impact, all other models were created without consideration of camber.

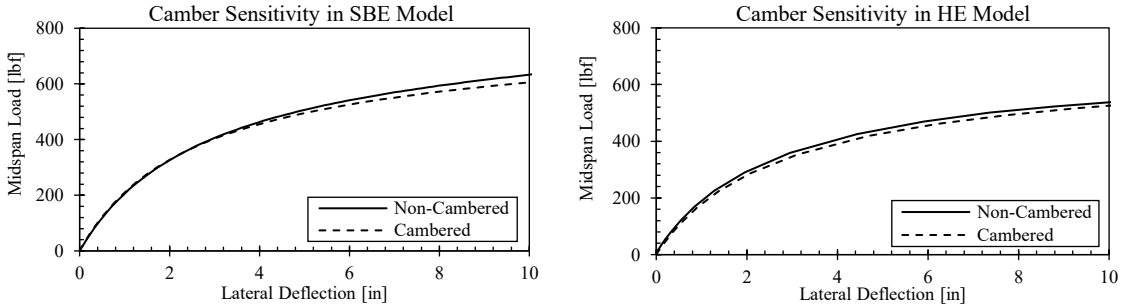

(a) (b)

Figure 8. Load-Deflection Plots for Camber Sensitivity for (a) the SBE Model and (b) the HE Model

4.3 Impact of Initial Sweep Imperfection

The initial sweep imperfection used when modelling LTB behavior is important as it affects both the stiffness of the element and its the critical buckling load. These values are typically given as a ratio of the element length (i.e., L/500), and are selected based on manufacturing tolerances, in-situ measurements, and verification with experimental results. The initial imperfection of the 32LH06 joist as measured by Schwarz (2002) at 1¾ in, was compared to the results of an upper and lower bound initial sweep of L/250 and L/1000, respectively. The load-lateral deflection curves for these initial sweep cases are presented in Fig. 9 (a) and (b) obtained from FEAs on the 32LH06 joist using the SBE and HE models, respectively.

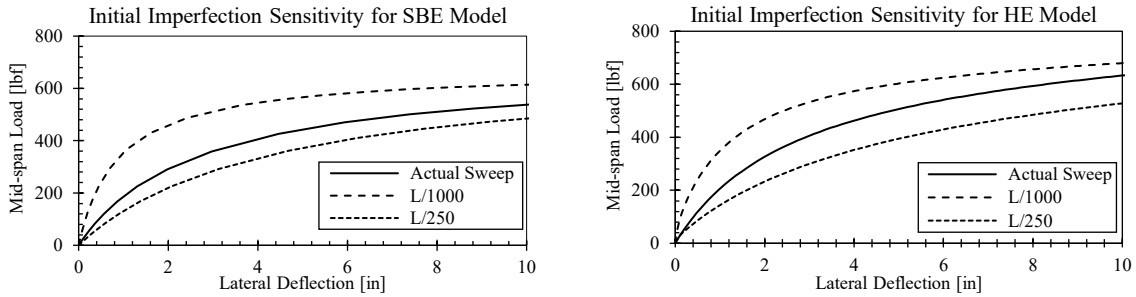

(a) (b)

Figure 9: Load-Deflection Plots for Variations of Initial Imperfections for the 32LH06 Joist (a) SBE Model and the (b) HE Model.

The results demonstrate that the initial sweep imperfection can have a substantial effect on the response. As such, it is important to properly capture the initial sweep imperfection in FEAs. Increased imperfection amplitude leads to reduced stiffness and lower predicted buckling capacity, consistent with the expected behavior. The measured imperfections from Schwarz (2002) for each joist were adopted for all subsequent analyses.

4.4 Impact of Filler Placement and Section Selection

Rojahn and Ziemian (2021) found that using filler elements with higher stiffness or a larger number of filler elements could result in a larger linear buckling capacity than those that used the recommended section of a 1-inch diameter rod section. A series of DBE models were created to evaluate the impact of the size and the number of filler elements on the response evaluation. In the first set of models, the size of the filler rod section was varied. In the second set of analyses, the number of filler elements was doubled in the model. The results from both sets of analyses are presented in Fig. 10 and compared with the baseline case with 1-inch fillers at locations shown in Fig. 2 (b).

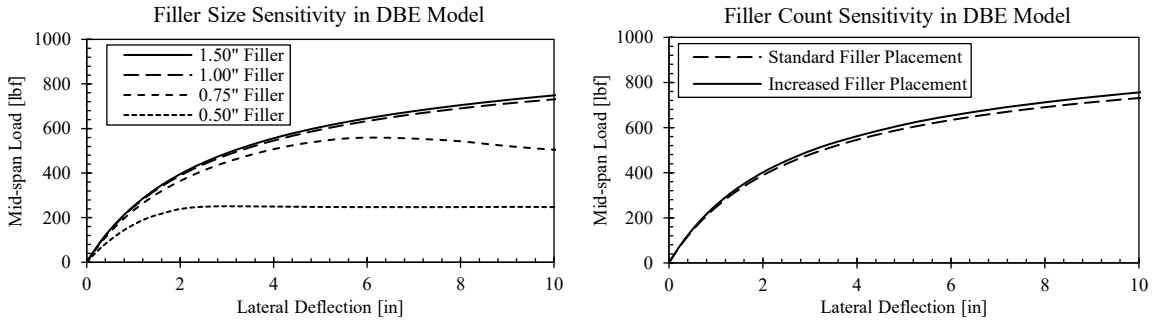

Figure 10: Load-Deflection Plots for Variations of (a) Filler Size and (b) Number of Fillers for 32LH06 DBE Model

The results show that the use of filler element profiles smaller than the recommended 1 in. diameter rod led to substantial reductions in predicted capacity. However, increasing the filler diameter beyond 1 in. resulted in only marginal increases in capacity. A similar trend was observed when increasing the number of filler elements. Based on these findings, the 1-inch diameter rod filler at locations shown in Figure 2 (b) was adopted for all subsequent DBE and HE models.

4.5 Impact of Coupling

Unlike beam-only formulations, HE shell/beam models require the definition of a kinematic coupling constraint between the beam-based filler elements and the shell-based chord elements. This coupling governs the transfer of forces and deformations between the two element types and represents a key modelling assumption. Three coupling configurations were examined, as shown in Fig. 11 (a). In the full-section coupling model, the filler node was coupled to the entire angle section within the shell chord. In the inside-section coupling model, coupling was restricted to the interior face of the angle section adjacent to the filler. In the proportional coupling model, only the portion of the interior face corresponding to the assumed contact region of the filler was coupled.

The coupling methodology significantly influenced the response despite being a relatively localized modelling assumption, as shown in Fig. 11 (b). Full-section coupling overestimated both stiffness and ultimate capacity compared to experimental results. Although the proportional

coupling approach was theoretically expected to provide the best match with experimental results, the inner coupling method provided the best match with experimental results. However, since boundary element stiffness effects were neglected in this study, the proportional coupling method likely represented the most realistic joist stiffness. Based on this analysis, proportional coupling was adopted for all subsequent HE models analyses of the remaining joist specimens.

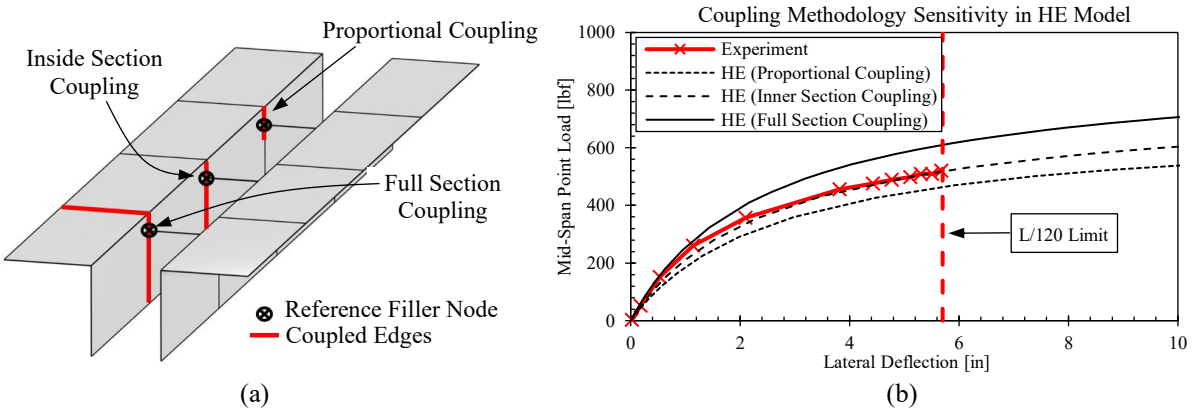

(a) (b)

Figure 11: (a) HE Model Chord-Filler Coupling Methodologies and (b) Load-Deflection Plot of Coupling Behavior

5. Results and Discussion

5.1 32LH06 Results

A summary of the result obtained from different models for the 32LH06 specimen are shown in Table 4 and Fig 12. The SBE model, the HE model with inner-section coupling, and the SE model with continuous filler were found to have the best agreement with the experimental results for the benchmark 32LH06 OWSJ, as shown in Fig 12. (a).

Table 4. Buckling capacities for the 32LH06 Joist at Lateral Deformation of 5.7 in

32LH06 Modelling Methodology	Linear Buckling Capacity (lbf)	Nonlinear Buckling Capacity (lbf)	Ratio to Experimental
Experimental Test	N/A	520.4	1.00
SBE	798.1	540.4	1.02
DBE (1" Filler Element)	809.3	659.6	1.20
HE (Proportional Coupling)	651.9	463.2	0.89
HE (Inner Section Coupling)	736.2	517.7	0.99
HE (Full Section Coupling)	831.8	610.4	1.17
SE	454.1	317.3	0.61
SE (Additional Fillers)	550.7	372.0	0.71
SE (Continuous Filler)	764.4	532.0	1.02

The SBE model provided a consistent baseline for evaluating the remaining modelling approaches and generally produced buckling capacities in reasonable agreement with the experimental results. Variations in the chord section definition influenced the predicted response, as shown in Fig. 12 (b). Placement of the linking segment near the shear center resulted in a higher predicted capacity, comparable to that obtained from the DBE model, where placement at the bottom of the section produced capacities that more closely matched the experimental results.

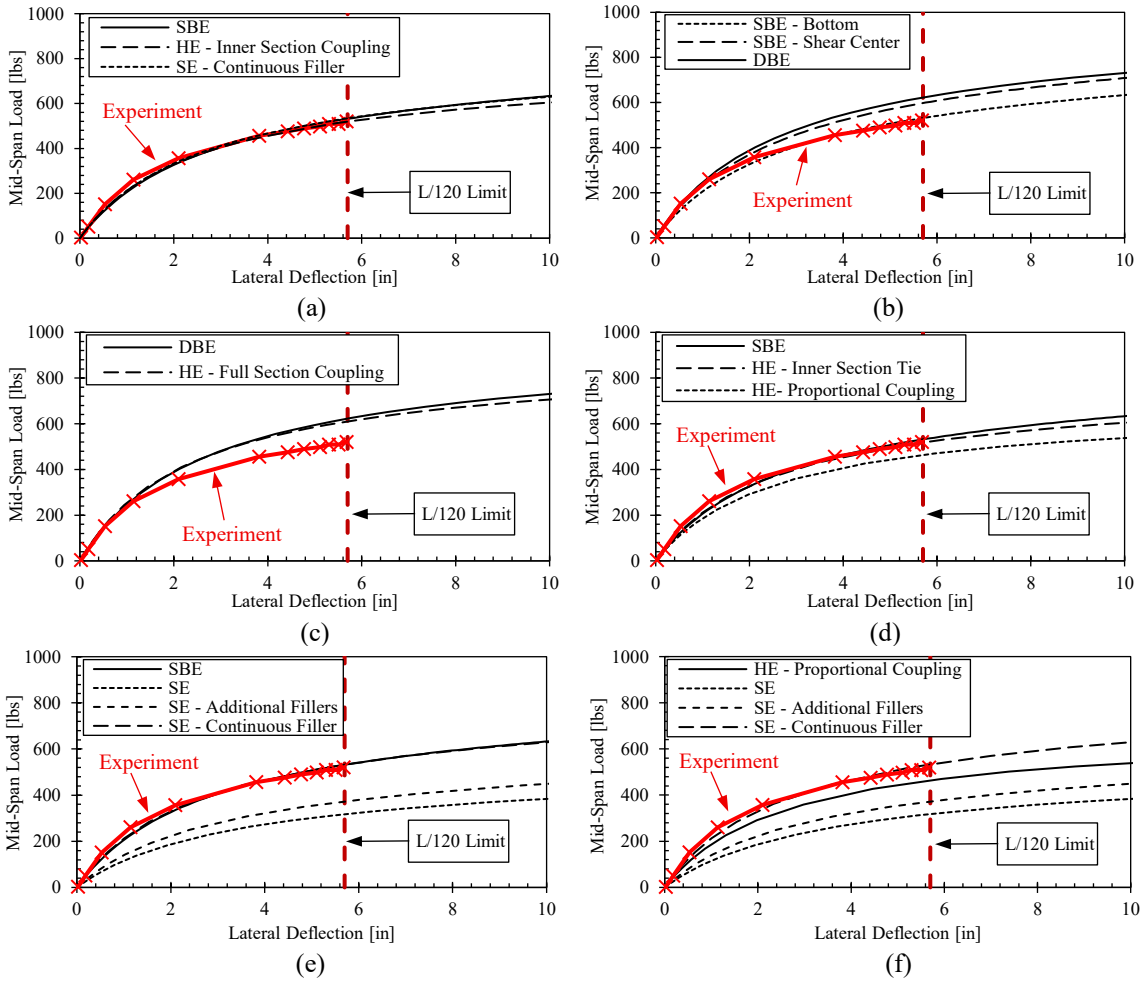

Figure 12: Nonlinear Analysis Results for 32LH06 OWSJ Model with Experimental Results from Schwarz (2002) in Red. Vertical Dashed Red Line Represents L/120 Deflection Limit

The DBE model produced substantial increases in lateral stiffness and predicted buckling capacity relative to the SBE model and experimental results, suggesting that modelled filler elements introduced unrealistically high rotational and translational restraint between chord components, leading to unconservative predictions. Because chord angles were modelled using beam elements, the filler effectively restrained the entire angle section, limiting internal distortion and contributing to elevated capacities. This interpretation was confirmed through observing a close agreement between results from the DBE model and results from the HE model with full-section coupling, as shown in Fig. 12 (c).

The remaining HE models exhibited closer agreement with experimental results and the SBE model. The inner-section coupling approach showed the closest agreement with experimental results, as illustrated in Fig. 12 (d). The HE model with proportional coupling predicted slightly lower buckling capacity, reflecting increased internal distortion permitted between parallel chord angles. This behavior was consistent with reduced rotational restraint from proportional coupling, which allowed more localized chord deformations compared to inner-section coupling, where shell chords behaved more rigidly.

The SE models generally exhibited the lowest stiffness and buckling capacity among modelling methodologies examined. Both the base SE model and the model with additional fillers at chord-web connections predicted capacities substantially lower than the SBE model and experimental results, as shown in Fig. 12 (e). This indicated that the SE formulation underpredicted the stiffness contribution of chord/web connections compared to beam-based filler representations. While some capacity reduction was expected due to less idealized behavior at the chord/web interface, predicted capacities were lower than those from the HE model with proportional coupling, as shown in Fig. 12 (f), suggesting that SE models may unrealistically underpredict global joist strength. In contrast, the SE model with continuous filler showed improved agreement with both the SBE model and experimental results, which further confirmed that the reduced capacity was primarily due to the reduced stiffness of the connections.

A common characteristic in all models representing chord angles as discrete elements is the shear lag behavior during LTB, shown in Fig. 13. This response is most evident in the DBE approach, where pronounced stress concentrations occur at filler element locations. Similar behavior appears in the HE and SE models, though stress discontinuities at filler locations are less severe and dissipate over shorter distances.

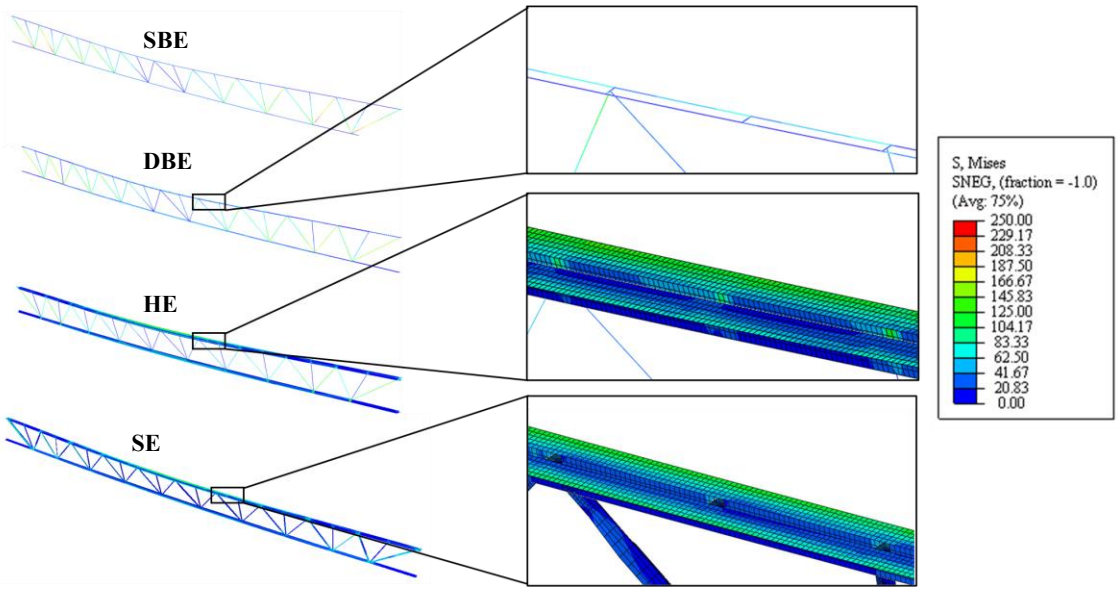

Figure 13: Stress Concentrations and Shear Lag Behavior within Each Modelling Methodology

5.2 Evaluation of Other Joist Models

For each of the remaining reference OWSJs, a limited set of models were developed based on observations from numerical simulations on the benchmark 32LH06 joist, described above. Initial geometric imperfections were included using the measured initial sweep values reported by Schwarz (2002). For the HE and DBE models, where applicable (i.e., OWSJs longer than 30') the two chord members were connected using filler elements defined as 1-inch-diameter rods. The computed capacities for each joist are summarized in Tables 5 – 8. Experimental results are not included in these comparisons as the absence of boundary element springs in the numerical models led to lower predicted capacities relative to those observed experimentally. As a result, direct comparison with test data provides limited insight into the relative effectiveness of the modelling methodologies considered.

Table 5. Buckling Capacities for the 10K1 Joist

10K1 Modelling Methodology	Linear Buckling Capacity (lbf)	Nonlinear Buckling Capacity (lbf)	Ratio to Single Beam Element
SBE	427.2	424.5	1.00
DBE (1" Filler Element)	478.8	469.6	1.11
HE (Proportional Coupling)	528.3	485.7	1.14

Table 6. Buckling Capacities for the 18K3 Joist

18K3 Modelling Methodology	Linear Buckling Capacity (lbf)	Nonlinear Buckling Capacity (lbf)	Ratio to Single Beam Element
SBE	281.0	258.6	1.00
DBE (1" Filler Element)	281.0	254.1	0.98
HE (Proportional Coupling)	292.3	252.0	0.97

Table 7. Buckling Capacities for the 26K5 Joist

26K5 Modelling Methodology	Linear Buckling Capacity (lbf)	Nonlinear Buckling Capacity (lbf)	Ratio to Single Beam Element
SBE	601.4	531.9	1.00
DBE (1" Filler Element)	663.2	581.6	1.09
HE (Proportional Coupling)	589.0	492.0	0.93

Table 8. Buckling Capacities for the 28K10 Joist

28K10 Modelling Methodology	Linear Buckling Capacity (lbf)	Nonlinear Buckling Capacity (lbf)	Ratio to Single Beam Element
SBE	556.4	387.2	1.00
DBE (1" Filler Element)	607.0	431.5	1.11
HE (Proportional Coupling)	557.5	372.7	0.96

The modelling results obtained for the remaining OWSJs highlight several consistent trends. As joist size and span increased, the differences among the modelling methodologies became more pronounced. The DBE approach generally predicted the highest buckling capacities, while the HE models produced the lowest capacities, with the SBE results typically falling between these bounds.

5.3 Discussion

The SBE model showed reasonable accuracy compared to experimental results while being simple and efficient to model. In addition, using the SBE model does not require specialized training or specialized finite element packages. However, this simplicity comes at a cost of potentially neglecting local effects that could affect the behavior of the joist. For instance, the SBE model simplifies the modelling of web/chord connections and cannot capture local buckling or warping effects. The SBE model may at times underpredict the capacity of the joist relative to the other modelling approaches, as seen with the 10K1 models. This is more likely to be the case for shorter span OWSJs with a smaller aspect ratio in joist section (smaller depth to width ratio), which results in a relatively stronger weak axis to strong axis bending capacity.

In contrast, the DBE model overpredicted the capacity of the 32LH06 joist, likely due to over-restraint imposed on the chord angles at the filler/chord connection. However, the same trend was

not observed for shorter joists. One benefit of the DBE methodology is that it allows each chord angle to act independently and accurately models the chord effective lengths, filler placement within the chords, and weak axis bending resistance. However, the filler stiffness still relies on assumptions related to the web/chord connection stiffness. Furthermore, the beam element chords in the DBE model do not allow for proper consideration of local effects or full control over the coupling behavior at the chord/filler locations.

The HE models also showed reasonable agreement with the experimental results, and the results of the SBE model. Similar to the DBE methodology, the HE method allows both chords to act independently but also enables effective consideration of local effects and more control over coupling behavior at filler/chord connections. However, the HE models still required an assumed filler section to replicate web/chord connection stiffness. A limitation of this assumption is that, even when proportional coupling is employed, the one-inch-diameter filler rod provides a relatively greater degree of restraint for smaller joists than for larger joists, since the chord dimensions vary with joist size while the filler geometry remains constant.

The SE modelling approach was only evaluated for the benchmark 32LH06 joist, however in that evaluation these models underpredicted the capacity of the joist. This is likely due to the reduced stiffness displayed by shell element webs when performing shear transfer between the two top chords. Even when filler elements were included, the tie connection between the chord and filler elements did not achieve the stiffness levels of the HE, SBE, or DBE models. It is likely that this underprediction is due to the exclusion of boundary condition effects in the model.

Given these factors, the HE model provided a reasonable balance between computational efficiency and accuracy. While the SBE model is more efficient to create, it lacks the flexibility provided by the HE model, which allows users to tailor parameters including filler size, placement, and coupling behavior.

It is important to note that these analyses were conducted without consideration of the impact of the non-idealized boundary conditions on the overall models. If these conditions were considered, the increased end stiffness would likely result in higher capacity for each model, aligning better with experimental results.

6. Conclusion and Recommendations

This study examined several different modelling methodologies for FEAs on OWSJs. Several models were developed including the use of beam elements to model the double angle chords as either a combined arbitrary section, or as two parallel sets of beam elements representing each chord and connected by fillers. Additional models using shell elements were also considered including the use of hybrid beam-shell and shell element models. Several secondary modelling parameters were investigated, including camber, initial imperfection, section definition, coupling methodology, and filler element placement. Finally, additional joists with various geometries were studied to identify if the joist geometry could affect the accuracy of results from different modelling approaches. The study leads to the following conclusions and recommendations for future work:

- When capturing the LTB capacity, without a concern for local effects such as local buckling, warping effects, and connection effects, SBE models are recommended given their efficiency.

- Where modelling efficiency is not a concern, HE or SE models could be used to fully capture the complex local behaviors such as local buckling, warping, shear lag near fillers, and restraint provided by the fillers.
- In addition to the overall modelling methodology, other modelling assumptions can have significant impact on the overall LTB capacity obtained from joist models, including the definition of the arbitrary, thin walled, double chord section for the SBE model, and the coupling methodology used for the HE models. When using the SBE modelling approach, it is recommended to model the thin connection segment at the bottom of the section.
- The inclusion of camber in FE models examining the lateral torsional buckling behavior of the joist has a minimal impact on the overall buckling capacity and is thus not recommended for future models.
- The initial sweep imperfection has a significant impact on the nonlinear buckling capacity and stiffness of joist models. Care should be taken to determine the most appropriate initial imperfection for analysis. Where possible, initial sweep imperfection must be physically measured.
- The relative impact of the use of each modelling procedure on the buckling capacity of the joist models varies based on the span, geometry, and member composition of each joist. Additional studies are required to further understand which modelling approaches are best suited for joists of different geometry,
- Future work is also recommended where the effects of boundary conditions are included in the FEAs, to further refine the most effective modelling methodologies for OWSJs.

References

Abaqus (2023). *Version 2023*. Dassault Systèmes Simulia Corp.

Cicek, K., Sputo, T., Blum, H.B. (2024). "The impact of analysis assumptions on buckling prediction in open-web steel joists." *Proceedings of the Annual Stability Conference, Structural Stability Research Council*, SSRC 2024.

Eberle, J.R., Ziemian, R.D., Potts, D.R. (2012). "Computational studies aimed at defining bridging requirements for steel joists." *Proceedings of the Annual Stability Conference, Structural Stability Research Council*, Grapevine, Texas, April 18–21, 2012.

Emerson, M.R. (2001). "Stability of Unbraced Steel Joists Subject to Mid-Span Loading." Master's Thesis, Bucknell University.

Galambos, T.V., "Bracing of Trussed Beams," SSRC Specialty Conference, IS YOUR STRUCTURE SUITABLY BRACED?, Milwaukee, WI, April, 1993

Moore, J.A. (2024). Diagonal Erection Bridging for Open Web Steel Joists with Flush Frame Connections. Master's Thesis, University of Tennessee.

Minkoff, R. M., Stability of Steel Joists During Erection, Research Report No. 39, Washington University, Aug. 1975

Rojahn, G.M.K., Ziemian, R.D. (2021). "Finite element modelling of open web steel joists comprised of nonsymmetric shapes." *Proceedings of the Annual Stability Conference, Structural Stability Research Council*, Louisville, Kentucky, April 13–16, 2021.

Schwarz, J.E. (2002). "Stability of Unbraced Steel Joists Subject to Mid-Span Loading," Phase II. Master's Thesis, Bucknell University.

Steel Joist Institute (2020). "Standard Specification for K-Series, LH-Series, and DLH-Series Open Web Steel Joists and for Joist Girders." Steel Joist Institute, Florence, South Carolina.

Strand7 (2020). Strand7 software, www.strand7.com

Ward, L.J. (2025). "A Numerical Investigation of Erection Bridging in Double-Pitched Open-Web Steel Joists." Master's Thesis, Utah State University.

Ziemian, R.D., Liu, SW., and McGuire, W. (2019) MASTAN2, www.mastan2.com.

Ziemian, R.D., Schwarz, J.E., Emerson, M.E., Potts, D.R. (2004). "Stability of unbraced steel joists subject to mid-span loading." *Proceedings of the Annual Stability Conference, Structural Stability Research Council,* Long Beach, California.